Catalysis Letters Vol. 109, Nos. 3–4, July 2006 (© 2006)
DOI: 10.1007/s10562-006-0075-1

Selective hydrogenation of benzene to cyclohexene over colloidal ruthenium catalyst stabilized by silica

Jianbo Ning, Jie Xu,* Jing Liu, and Fang Lu

State Key Laboratory of Catalysis, Dalian Institute of Chemical Physics, Graduate School of the Chinese Academy of Sciences, 457 Zhongshan Road, 110, Dalian 116023, P.R. China

Received 18 January 2006; accepted 25 January 2006

A colloidal ruthenium catalyst stabilized by silica was prepared through microemulsion processing. Ruthenium colloids with particle size about 4 nm are highly dispersed in silica. The selective hydrogenation of benzene to cyclohexene was studied over the catalyst. Much higher activity and selectivity was obtained compared with its supported counterparts.

KEY WORDS: benzene; selective hydrogenation; cyclohexene; microemulsion; ruthenium; colloids; silica.

1. Introduction

Cyclohexene is an important intermediate material for producing nylon6, nylon66, and fine chemicals, etc. Thus, the preparation of cyclohexene has attracted great research interest academically and industrially. Among various synthetic routes, such as cyclohexanol dehydration, cyclohexane halide dehydrohalogenation, cyclohexane dehydrogenation and so on [1–3], selective hydrogenation of benzene to cyclohexene (SHBC) receives much attentions due to economical requirements and environmental considerations [4–6].

Ruthenium has been found the most efficient catalyst for the process of SHBC among transitional metal catalysts, such as Ru [4], Pt [7], Rh [8–10], Ni [11] and rare earth *et al*. [12,13]. With alcohol as additive, Hartog *et al*. first obtained 2% yield of cyclohexene with ruthenium catalyst in hydrogenation of benzene under liquid-phase [14]. Under aqueous solution of zinc salts, over 30% yield of cyclohexene can even be achieved over ruthenium catalyst [15]. However, the activities of ruthenium catalysts are rather low due to large amount of adsorption of water on ruthenium sites [5,16,17].

Nanoparticles(colloids), due to their large surface-to-volume ratio, offer higher catalytic efficiency per gram than larger sized materials [18]. As efficient catalysts, stabilized nanoparticles(colloids) have been widely used for hydrogenation, coupling and so on. For example, rhodium nanoparticles stabilized by the ionic copolymer showed unprecedented lifetime and activity in arene hydrogenation under forcing conditions [19]; Pd nanoparticles immobilized in ionic liquid are efficient catalyst precursors for coupling of aryl halides with *n*-butylacrylate [20]; dendrimer-encapsulated Pd nanoparticles are effective catalysts for coupling aryl halides to organostannanes (the Stille reaction) under mild conditions [21]. However, there are rather few researches on the preparation and evaluation of nano-colloidal ruthenium catalyst used in SHBC in the literature to the best of our knowledge.

In the present study, colloidal ruthenium catalyst stabilized by silica (RuC1) is synthesized through microemulsion processing. The nature of the as-prepared catalyst is characterized by transmission electron spectroscopy (TEM), X-ray diffraction (XRD), and X-ray photoelectron spectroscopy (XPS). The catalytic performances on SHBC are further investigated and compared with supported ruthenium catalysts. Meanwhile, SHBC variables, such as the temperature, the stirring rate, and the pressure are optimized.

2. Experimental

2.1. Materials

Tetraethylorthosilicate (TEOS) and cyclohexane (>99%) were purchased from Tianjin Kermel Chemical Reagent Development Center; $RuCl_3 \cdot 3H_2O$ (35–38%) was purchased from Shenyang Reaserch Institute of Nonferrous Metals; $ZnSO_4 \cdot 7H_2O$ (>99%) was purchased from Shanghai Jinshan Chemical Plant; Poly (oxyethylene) nonylphenol ether (NP-7) was purchased from Dalian chemical ctl.; Silica (100 meshes, $Sg = 200\ m^2\ g^{-1}$) was purchased from Institute of Oceanology, Chinese Academy Science; KBH_4 (>98%) was purchased from Tianjin Fuchen Chemical Reagent Factory.

*To whom correspondence should be addressed.
E-mail: xujie@dicp.ac.cn

2.2. Catalyst preparation

A typical preparation of colloidal ruthenium catalyst stabilized by silica (RuC1), involving silica *in situ* formed in microemulsion, is as follows. Firstly, two microemulsions were prepared. Microemulsion-A contained 50 mL cyclohexane as oil phase, 8.0 g NP-7 as surfactant and 1.6 mL ruthenium trichloride (0.36 M) aqueous solution; Microemulsion-B contained 50 mL cyclohexene, 8.0 g NP-7 and 1.6 mL KBH_4 (1.39 M) aqueous solution. Secondly, microemulsion-B was added into microemulsion-A, and the mixture turned deep brown green. Then, TEOS and ammonium aqueous solution (4.0 M) were charged into the microemulsion under continuous stirring, and the hydrolysis of TEOS was performed at 303 K for 12 h. The gel was recovered by adding 50 mL acetone and centrifugation, then washed by ethanol and distilled water in order to remove the surfactant. The surfactant was removed as determined by FT-IR spectroscopy. Before catalysts test, the catalysts were pretreated in 120 mL of 0.6 M zinc sulfate for 12 h under 413 K, 6.0 MPa of hydrogen pressure, then washed with 100 mL water and finally they were stored in absolute ethanol.

RuS1 preparation was similar to RuC1, except that microemulsion-A was firstly mixed with 0.75 g commercial silica as silica source (100 meshes, Sg = 2 00 $m^2\ g^{-1}$).

The RuS2 sample was prepared in traditional methods [22] and then pretreated in the same way as RuC1 before reaction.

2.3. Catalyst characterization

The morphology of the sample was observed through a transmission electron microscopy (TEM) on a JEOL JEM 2000EX electron microscope at an accelerating voltage of 200 kV.

Powder X-ray diffraction patterns (XRD) of the samples were carried out on a Magix (PANalytical) powder diffraction instrument. The operation parameters were: Cu K_α radiation, Ni filter, 50 mA, 100 kV, 2θ scanning from 20 to 80° with a step size of 0.02.

X-ray photoelectron spectroscopy (XPS) measurements were made using an Amicus (Kratos) equipment, taken as reference the C1s signal at 284.7 eV. Determinations of the superficial atomic ratios were made by comparing the areas under the peaks after background subtraction and corrections due to differences in escape depth an in photoionization cross-sections.

Fourier transform infrared (FT-IR) spectroscopy was performed on a Bruker Tensor 27 FT-IR spectrometer with 32 scans for a resolution of 4 cm^{-1} in KBr media at room temperature.

2.4. Catalytic measurements

The selective hydrogenation of benzene over Ru catalysts was carried out in a 500 mL stainless autoclave with a mechanical stirrer. After 120 mL of 0.6 M $ZnSO_4$ was added, the as-prepared catalyst and 60 mL benzene were introduced. Then the autoclave was sealed and purged with N_2 for more than five times to exclude air. The process was monitored by taking small amounts of the mixture solution at intervals, followed by Agilent 4890 GC gas chromatograph with a flame ionization detector. An OV-101 capillary column (30 m × 0.32 m m × 0.8 um) was used for separation of product.

3. Results and discussion

3.1. Characterizations of catalysts

Figure 1 shows the TEM micrographs of RuC1 (figure 1b), RuS1 (figure 1c), and RuS2 (figure 1a). For RuC1, it reveals that small-sized ruthenium colloids are almost single dispersed in silica, and the average particle size of ruthenium is about 4 nm. For RuS1, ruthenium colloids are dispersed in size and tend to be agglomerated on the external surfaces of silica. When it comes to

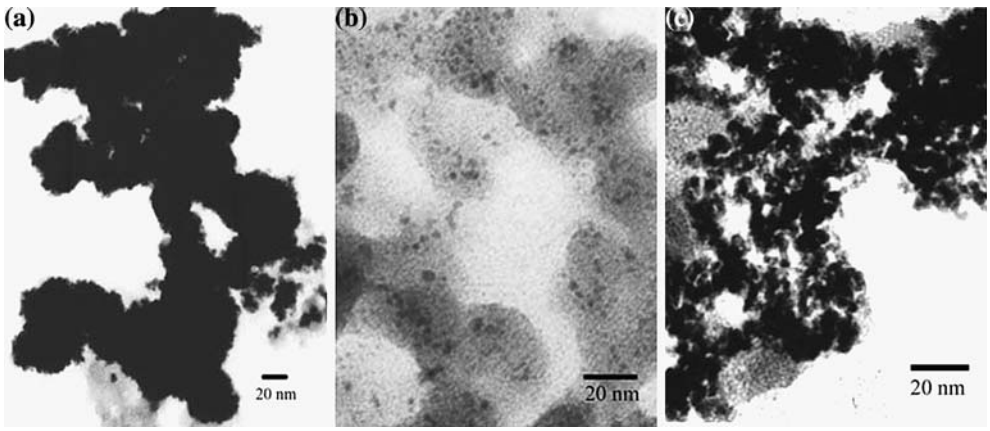

Figure 1. TEM of the samples: (a) RuS2, (b) RuC1, (c) RuS1.

RuS2, ruthenium colloids are agglomerated and covered almost all the surface of silica. The different results may be bring by various deposition processing. For RuC1, ruthenium particles are first formed in water droplets of microemulsion which controls the final size of the particles [23,24], and then the silica *in situ* formed in microemulsion is filled in the blank of the particles and keeps the nanoparticles of ruthenium from aggregating after surfactant removed. Thus, small-sized ruthenium colloids are well dispersed in silica for RuC1. For RuS1, although the formation of ruthenium colloids on silica are protected by surfactant in microemulsion, they tend to be aggregated on the surface of silica after surfactant is removed. When it comes to RuS2, the pores of the silica were first filled with $RuCl_3$, and the deposition of ruthenium particles by adding KBH_4 solution then occurred accompanied by the release of hydrogen. The Ru particles can be pushed out by hydrogen and aggregated on the external surface of silica.

The XRD patterns of the samples further reveal the small-sized ruthenium colloids in RuC1 (figure 2, line b). A peak around $2\theta = 22°$, which results from the amorphous silica support [22], is clearly observed. However, the peak around $2\theta = 43°$, which can be ascribed to Ru [25], is very weak for RuC1. It indicates the size of Ru colloids is so small that it is difficult to be detected by this method. For RuS1(figure 2, line c), a very weak peak around $2\theta = 43°$ is also observed though some ruthenium colloids aggregated. It proves that the size of ruthenium colloids is also very small. However, the peak of ruthenium is much stronger for RuS2 (figure 2, line a) compared with those of RuC1 and RuS1. It indicates that the size of ruthenium colloids by traditional methods is much bigger than that prepared from microemulsion processing. In addition, nearly all the Ru species are present in the metallic state corresponding to two XPS peaks at binding energy (BE) of 280.4 eV in $Ru3d_{3/2}$ and 284.6 eV in $Ru3d_{5/2}$ levels, and no boron is detected.

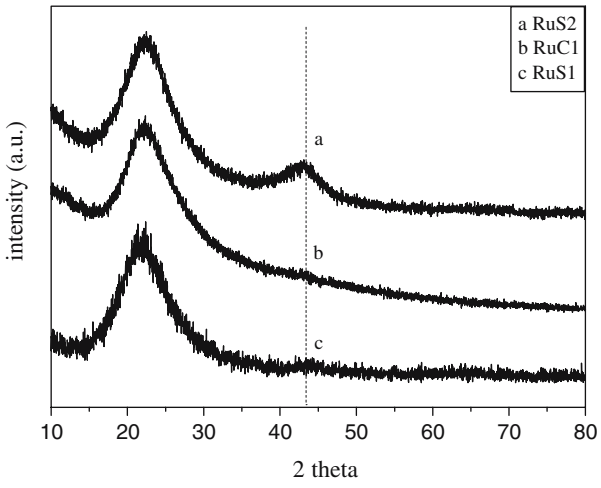

Figure 2. XRD patterns of the samples prepared by different methods.

3.2. Activation behaviors

3.2.1. The effect of catalyst preparation methods on selective hydrogenation of benzene

Table 1 shows the maximum yield of cyclohexene and the corresponding time, conversion of the benzene and activity of different catalysts. The maximum yield of cyclohexene is 42.2, 3.0, and 2.1% for RuC1, RuS1, and RuS2, respectively. The TOF are 0.80, 0.76, and 0.08 S^{-1} for RuC1, RuS1, and RuS2, respectively. The activities of RuC1 and RuS1 were compatible, and were much higher than that of RuS2. This can be attributed to much smaller size of Ru colloids of RuC1 and RuS1 compared with that of RuS2. As shown in figure 1, the size of ruthenium for RuC1 is about 4 nm. For RuS1, some ruthenium colloids are aggregated, but the size of ruthenium is very small which can be proved from XRD. On the other hand, much bigger sized ruthenium colloids for RuS2 is observed from TEM and XRD. Because small sized nanoparticles give larger surface-to-volume ratio per gram than larger sized materials and expose more active sites [18,26], much higher activity is reasonably achieved over RuC1 and RuS1 than that over RuS2. It should be noted that RuC1 also gives a noticeable selectivity to cyclohexene. Here, the superior selectivity towards cyclohexene over the RuC1 catalyst might attribute to much higher content of surface hydroxyl groups on silica *in situ* formed, which is expected to enhance greatly the hydrophilicity of the catalyst. Because water molecules adsorb on the active ruthenium sites where the cyclohexane is preferentially formed, and it promote the desorption of cyclohexene by a competitive adsorption or by the formation of an adduct with cyclohexene, the increasement of hydrophility benefits benzene hydrogenation to cyclohexene [2,5,16, 17]. In addition, dispersed morphology of RuC1 may also contribute its much higher selectivity, because cyclohexene readsorption may become much difficult in the channel composed of ruthenium and silica compared with that composed only of ruthenium before they escape into oil phase through water layer.

Table 1
Performance of samples for benzene hydrogenation to cyclohexene[a]

Samples	Time (min)	Conversion (%)	Selectivity (%)	Yield (%)	TOF[b] (s^{-1})
RuS2	100	14	15	2	0.08
RuS1	25	36	9	3	0.76
RuC1	40	68	63	42	0.80

[a]Reaction condition: 413 K, 6.0 MPa, 1000 rpm, 60 mL benzene and 120 mL of 0.6 M aqueous of $ZnSO_4$. [b]The catalyst activity was expressed in terms of turnover frequency (TOF, s^{-1}) calculated as the ratio of the concentration of benzene consumed per unit time to the concentration of the total metal.

3.2.2. The effect of reaction temperature on selective hydrogenation of benzene

Figure 3a shows that the effect of reaction temperature upon the selectivity and yield of cyclohexene over RuC1. As the reaction temperature is elevated from 403 to 433 K, both selectivity and yield of cyclohexene increases firstly, however, the selectivity and the yield of cyclohexene slight decrease in still higher temperature more than 413 K. It can be explained by the viewpoint of Struigk *et al*. [27,28]: Elevating reaction temperature facilitates desorption of cyclohexene, at the same time, the surface coverage of hydrogen is lowered, which reduces the rate for further cyclohexene hydrogenation. While on the other hand, elevating reaction temperature could also enhance the solubility of cyclohexene in the stagnant water film surrounding the catalyst, which would increase the surface coverage of cyclohexene and so the cyclohexene hydrogenation rate. Such an effect counteracts with the positive effects mentioned above, and above 413 K, it becomes dominant and brings about the deviation from the upward trend of cyclohexene yield with respect to temperature. When the reaction temperature is elevated within the investigated range, the conversion of benzene also tends to increase, similar phenomenon was also reported by J. Wang *et al*. [28].

3.2.3. The effect of hydrogen pressure on selective hydrogenation of benzene

Figure 4 shows the effect of hydrogen pressure upon the yield and selectivity of cyclohexene over RuC1. It can be seen that the selectivity of cyclohexene increases with elevating pressure from 4.0 to 6.0 MPa, and decreases slightly when hydrogen pressure increases to 7.0 MPa. The result indicates that there is an optimum pressure which gives the highest yield of cyclohexene.

The phenomenon can be ascribed to two effects: The routes of hydrogenation of benzene are influenced by hydrogen pressure; the rates of all the individual hydrogenation steps are different functions of the hydrogen pressure.

According to Prasad [29] and Ronchin [30], hydrogenation of benzene is mainly through two reaction routes: (i) A planar π complex of benzene undergoes a step hydrogenation via linear σ-bonded benzene (S sites type) in the presence of two hydrides bonded in different catalyst sites (the consecutive mechanism). (ii) A planar π complex of benzene is displaced in one step by six hydrides with a formation of a van der Waals adduct followed by complete hydrogenation to cyclohexane. The first mechanism is predominant at low molar ratio of benzene, and the second one becomes more important at higher benzene pressure. Cyclohexene can be obtained when hydrogenation of benzene is carried out in water through the consecutive mechanism. In the process, water competes with cyclohexene on surface adsorption disfavor its hydrogenation to cyclohexane. Accordingly, improving hydrogen pressure will decrease benzene partial pressure on the surface of ruthenium. Thus, it benefits hydrogenation of benzene through the step mechanism. Under low hydrogen pressure, improving hydrogen pressure will benefit selective hydrogenation of benzene to cyclohexene as a result of increasing hydrogenation of benzene through the step mechanism. However, the rate of cyclohexene hydrogenation to cyclohexane will also increase when there is an excessive amount of hydrogen on the surface. As a result, the selectivity of cyclohexene will decline in rather high hydrogen pressure.

On the other hand, the rates of all the individual hydrogenation steps will change with the hydrogen pressure. According to the consecutive hydrogenation mechanism[2,22,28], the rate of benzene to cyclohexene will increase gradually with an increase in the hydrogen pressure to the maximum point corresponding to the optimal surface coverage of benzene and hydrogen. However, at higher hydrogen pressure, a lower portion of empty active sites available for benzene will render a lower hydrogenation rate for benzene. At the same time, cyclohexene is easily hydrogenated to cyclohexane when there is an excessive amount of hydrogen on the surface. Our result revealed that the selectivity of cyclohexene at

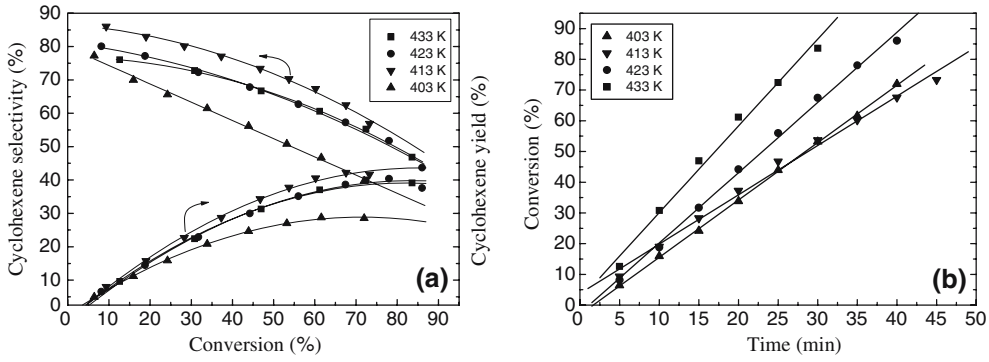

Figure 3. Effect of reaction temperature in hydrogenation of benzene to cyclohexene over RuC1: (a) Effect of temperature on the yield and selectivity to cyclohexene; (b) Effect of temperature on the reaction conversion. Reaction condition: 6.0 MPa, 1000 rpm, 60 mL benzene, 120 mL of 0.6 M aqueous of $ZnSO_4$.

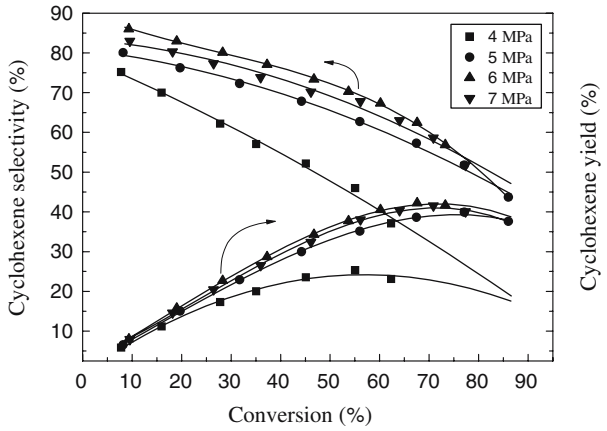

Figure 4. Effect of hydrogen pressure in hydrogenation of benzene to cyclohexene over RuC1. Reaction condition: 413 K, 1000 rpm, 60 mL benzene, 120 mL of 0.6 M aqueous of $ZnSO_4$.

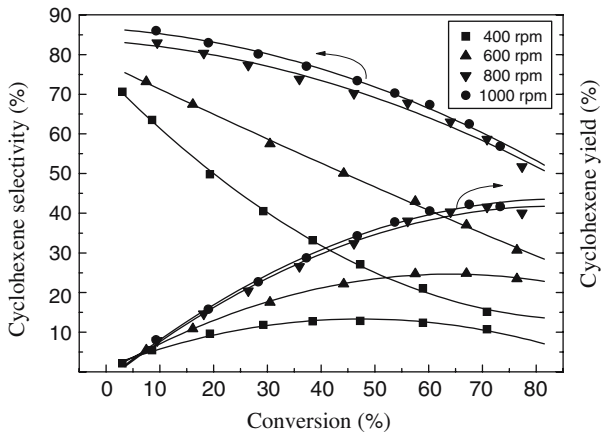

Figure 5. Effect of stirring rate in hydrogenation of benzene to cyclohexene over RuC1. Reaction condition: 413 K, 6.0 MPa, 60 mL benzene, 120 mL of 0.6 M aqueous of $ZnSO_4$.

6.0 MPa is greater than those at 4.0, 5.0 and 7.0 MPa, lending further support to above interpretation.

3.2.4. The effect of stirring rate on selective hydrogenation of benzene

Because stirring rate influences both the gas–liquid and the liquid–liquid interfacial areas, and thus affects the hydrogenation rate and the selectivity to cyclohexene. The effects of stirring rate on the cyclohexene selectivity, benzene conversion and catalyst turnover in the benzene hydrogenation are further investigated. As shown in figure 5, the selectivity of cyclohexene increases evidently when stirring rate is elevated from 400 to 800 rpm. Above 800 rpm, the cyclohexene selectivity increased not obviously, and benzene hydrogenation rate increases slightly according to our results (not shown here). The effects of stirring rate on the cyclohexene yield and on the benzene hydrogenation rate are in accordance with previous works[27,28].

4. Conclusion

A colloidal ruthenium catalyst stabilized by silica was prepared by employing microemulsion processing. Ruthenium colloids with particle size about 4 nm are highly dispersed in silica. It showed much higher activity and selectivity for selective hydrogenation of benzene to cyclohexene compared with its supported counterparts. The high selectivity can be attributed to high dispersion of ruthenium particles in silica decreasing the readsorption of cyclohexene on ruthenium sites. The remarkable hydrogenation rate can be attributed to highly dispersion of much small ruthenium colloids, exposing more active sites for benzene hydrogenation. An optimal reaction temperature and hydrogen pressure appeared on 413 K, 6.0 MPa, and >800 rpm.

References

[1] A.G. Shastri, J. Schwank and S. Galvagno, J. Catal. 100 (1986) 446.
[2] S.C. Hu and Y.W. Chen, J. Chem. Technol. Biotechnol. 76 (2001) 954.
[3] V. Mazzieri, F. Coloma-Pascual, A. Arcoya, P. L'Argentiere and N.S. Figoli, Appl. Surf. Sci. 210 (2003) 222.
[4] C. Milone, G. Neri, A. Donato and M.G. Musolino, J. Catal. 159 (1996) 253.
[5] L. Ronchin and L. Toniolo, Catal. Today 66 (2001) 363.
[6] E.T. Silveira, A.P. Umpierre, L.M. Rossi, G. Machado, J. Morais, G.V. Soares, I.L.R. Baumvol, S.R. Teixeira, P.F.P. Fichtner and J. Dupont, Chem.-Eur. J. 10 (2004) 3734.
[7] H. Ichihashi and H. Yoshioka, J P 62142126 (1987).
[8] O.L.A.C. Marina and C. Paniel, J. Mol. Catal. 39 (1987) 341.
[9] E. Galicia, G. Diaz and S. Fuentes, Stud. Surf. Sci. Catal. 38 (1987) 11.
[10] S. Galvagno, A. Donato, G. Neri and D. Pietropaolo, React. Kinet. Catal. Lett. 37 (1988) 443.
[11] E. Dietzsch, U. Rymsa and D. Honicke, Chem. Eng. Technol. 22 (1999) 130.
[12] H. Imamura, T. Nuruyu, T. Kawasaki, T. Teranishi and Y. Sakata, Catal. Lett. 96 (2004) 185.
[13] H. Imamura, T. Kumai, K. Nishimura, T. Nuruyu and Y. Sakata, Catal. Lett. 82 (2002) 69.
[14] F. Hartog, J. Catal. 2 (1963) 79.
[15] W.C. Drinkard, NL 7205832 (1972).
[16] J. Struijk, M. Dangremond, W.J.M. Lucasderegt and J.J.F. Scholten, Appl. Catal. A 83 (1992) 263.
[17] J.A. Don and J.J.F. Scholten, Appl. Catal. 41 (1981) 146.
[18] S. Kidambi, J. Dai, J. Li and M.L. Bruening, J. Am. Chem. Soc. 126 (2004) 2658.
[19] X.D. Mu, J.Q. Meng, Z.C. Li and Y. Kou, J. Am. Chem. Soc. 127 (2005) 9694.
[20] C.C. Cassol, A.P. Umpierre, G. Machado, S.I. Wolke and J. Dupont, J. Am. Chem. Soc. 127 (2005) 3298.
[21] J.C. Garcia-Martinez, R. Lezutekong and R.M. Crooks, J. Am. Chem. Soc. 127 (2005) 5097.
[22] S.H. Xie, M.H. Qiao, H.X. Li, W.J. Wang and J.F. Deng, Appl. Catal. A 176 (1999) 129.
[23] I. Capek, Adv. Colloid Interface Sci. 110 (2004) 49.
[24] S. Eriksson, U. Nylen, S. Rojas and M. Boutonnet, Appl. Catal. A 265 (2004) 207.
[25] J.Q. Wang, P.J. Guo, S.R. Yan, M.H. Qiao, H.X. Li and K.N. Fan, J. Mol. Catal. A 222 (2004) 229.
[26] B.Z. Zhan, M.A. White, T.K. Sham, J.A. Pincock, R.J. Doucet, K.V.R. Rao, K.N. Robertson and T.S. Cameron, J. Am. Chem. Soc. 125 (2003) 2195.

[27] J. Struijk and J.J.F. Scholten, Appl. Catal. A 82 (1992) 277.
[28] J.Q. Wang, Y.Z. Wang, S.H. Zhe, M.H. Qiao, H.X. Li and K.N. Fan, Appl. Catal. A 272 (2004) 29.
[29] K.H.V. Prasad, K.B.S. Prasad, M.M. Mallikarjunan and R. Vaidyeswaran, J. Catal. 84 (1983) 65.
[30] L. Ronchin and L. Toniolo, Appl. Catal. A 208 (2001) 77.